A multiscale constitutive model for intergranular stress corrosion cracking in type 304 austenitic stainless steel

2013 J. Phys.: Conf. Ser. 451 012022

(http://iopscience.iop.org/1742-6596/451/1/012022)

A multiscale constitutive model for intergranular stress corrosion cracking in type 304 austenitic stainless steel

A Siddiq[1,2] and S Rahimi[1]

[1] Advanced Forming Research Centre (AFRC), 85 Inchinnan Drive, Glasgow, UK
[2] Department of Design, Manufacture and Engineering Management, University of Strathclyde, Glasgow, UK
Email: muhammad.amir@strath.ac.uk

Abstract. Intergranular stress corrosion cracking (IGSCC) is a fracture mechanism in sensitised austenitic stainless steels exposed to critical environments where the intergranular cracks extends along the network of connected susceptible grain boundaries. A constitutive model is presented to estimate the maximum intergranular crack growth by taking into consideration the materials mechanical properties and microstructure characters distribution. This constitutive model is constructed based on the assumption that each grain is a two phase material comprising of grain interior and grain boundary zone. The inherent micro-mechanisms active in the grain interior during IGSCC is based on crystal plasticity theory, while the grain boundary zone has been modelled by proposing a phenomenological constitutive model motivated from cohesive zone modelling approach. Overall, response of the representative volume is calculated by volume averaging of individual grain behaviour. Model is assessed by performing rigorous parametric studies, followed by validation and verification of the proposed constitutive model using representative volume element based FE simulations reported in the literature. In the last section, model application is demonstrated using intergranular stress corrosion cracking experiments which shows a good agreement.

1. Introduction

Austenitic stainless steels due to their superior corrosion resistance, excellent mechanical properties and good weldability have consistently been used in power generation plants and oil and gas industries [1–3]. Intergranular stress corrosion cracking (IGSCC) is a dominant failure mechanism in sensitized austenitic stainless steels subjected to critical environments where intergranular cracks extend along susceptible grain boundaries. Sensitization refers to the precipitation of chromium carbides at grain boundaries which is accompanied by the depletion of chromium in the vicinity of these regions and therefore susceptibility to IGSCC [4–7]. The susceptibility to sensitization and the kinetics of sensitization are strongly dependent on the geometry and crystallographic structure of the boundaries [8]. Grain boundary structure has commonly been classified in the framework of coincidence site lattice (CSL) model, which attributes a Σ (sigma) notation to each grain boundary. This describes the orientation relationship between the crystal lattices of the adjoining grains in the grain boundary and can be obtained using two-dimensional electron back scattered diffraction (EBSD) technique [9]. Based on the CSL model grain boundaries are often classified into two groups of low sigma ($\Sigma \leq 29$) and random ($\Sigma > 29$) or high angle grain boundaries. High angle grain boundaries ($\Sigma > 29$) that are frequently been referred to as random boundaries have higher susceptibility to sensitization than those with low sigma [10,11]. It has been observed that under similar mechanical loading and environment

conditions, intergranular cracks have tendency to propagate more slowly in microstructure with higher fraction of low Σ (Σ ≤ 29) boundaries [12]. From the correlation between intergranular crack path and boundary characters it can be deduced that random grain boundaries are more prone to chromium carbide precipitation while low Σ boundaries show more resistance [8,12,13]. Generally, coherent twin boundaries with a {111} habit pane have been found to be the only resistant feature to sensitisation phenomenon [8,13].

Several predictive methods have been developed to define the relations between intergranular crack propagation and the grain boundary properties. These predictive approaches determine the probability if crack arrest and distribution of arrested crack lengths for a given microstructure. These models can be categorized into percolation based models [10,11,14–30] and mechanics based modeling approaches [31–35]. Most of these predictive models were either analytical or FE based which require high amount of computational power and time.

In this study, a multiscale constitutive model has been presented for intergranular stress corrosion crack propagation in metals with emphasis on type 304 austenitic stainless steel. The presented model is computationally robust as it is based on homogenization technique and will save ample amount of computational time and resources. The proposed constitutive model takes into account the material's microstructure character distribution (GBCD) such as grain size and fraction of boundaries with different characteristics obtained by EBSD, and predicts the maximum intergranular crack length. The constitutive model assumes each grain to be a two phase material comprising of grain interior and grain boundary zone. Grain interior is modeled using crystal plasticity theory while grain boundary zone is modeled by proposing a phenomenological constitutive model motivated from cohesive zone modeling approach. Overall, the response of representative volume is calculated by volume averaging the individual grain behavior. In the first part of this paper, a brief outline of the constitutive model is discussed. In the second section, the validations and verification of the proposed constitutive model is presented by comparing with representative volume element based FE simulations reported in the literature. In the last section, model application is demonstrated using post-mortem stress corrosion experiments.

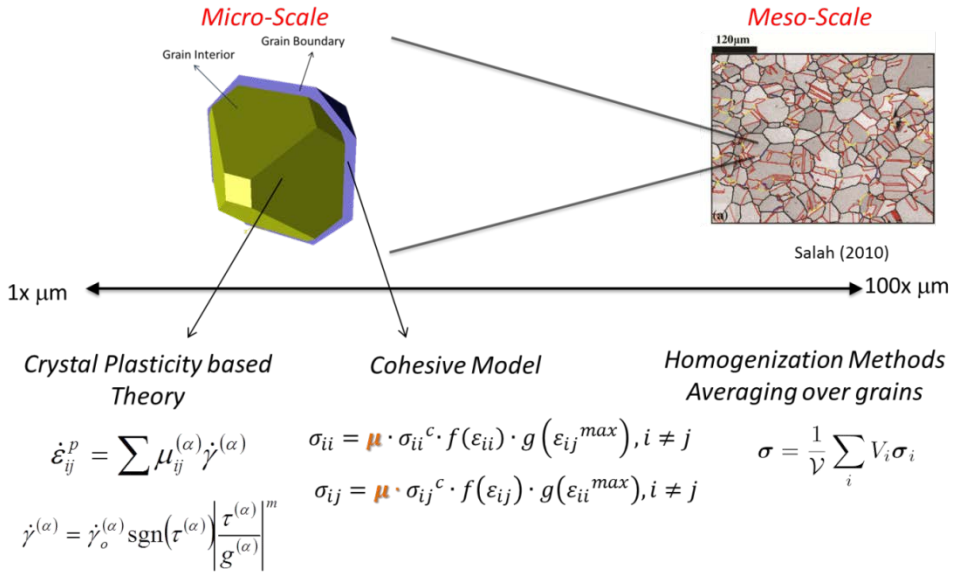

Figure 1. Schematic of multiscale constitutive model showing how scales are bridged.

2. Constitutive model

A brief outline of the constitutive model is discussed in the following. A detailed description of the model and implementation will be reported later in a full journal article. The grain structure is assumed to be truncated octahedron or Kelvin cell with 14 faces comprising of 6 hexagons and 6

tetragons. Each individual grain is considered as a two-phase material consisting of grain interior and the grain boundary zone as a thin shell (4 μm) encompassing the grain interior. Grain interior is modeled using crystal plasticity theory [36–42] while the grain boundary zone is modeled using a phenomenological constitutive model motivated from cohesive zone modeling approaches (please see references there in [36–42]). Schematic of the constitutive model is shown in Figure 1.

In the following we only present details of the calculation of overall response of the grain and a brief description of the models for both grain interior and grain boundary zone.

The stress conjugate to strain before fracture initiation is given by

$$\boldsymbol{\sigma} = \xi \boldsymbol{\sigma}_{gi} + (1-\xi)\boldsymbol{\sigma}_{gb}$$

where ξ is the volume fraction of the grain interior region and is given by

$$\xi = \frac{V_{gi}}{V_{gb}}$$

where σ_{gl} and σ_{gb} are the stresses in the grain interior and grain boundary zone. V_{gl} and V_{gb} are volume fractions of grain interior and grain boundary zone, respectively.

Each phase, i.e. grain interior and grain boundary zone are assumed to have same deformation gradient

$$\boldsymbol{F} = \boldsymbol{F}_{gb} = \boldsymbol{F}_{gi}$$

Once the crack is initiated stresses are computed using the following relation

$$\boldsymbol{\sigma} = \xi \cdot \frac{e^{1-\varsigma \cdot tanh\left(\frac{\varepsilon_{ij}-\mu\varepsilon_{ij,1}}{\mu(\varepsilon_0-\varepsilon_{ij,1})}\right)^2}}{2.718} \cdot \boldsymbol{\sigma}_{gi} + (1-\xi)\boldsymbol{\sigma}_{gb}$$

The first term of the above equation accounts for unloading of the grain interior instantly after the initiation of a crack, i.e. when the crack propagation starts. Where μ and ζ can be estimated from experiments. ζ controls the damage evolution and μ links directly the rise in normalised impurity concentration with drop in strength and strain to failure.

Polycrystalline response is computed using classical Taylor type averaging method. The homogenized stress response is computed through arithmetic averaging of overall grains.

$$\bar{\boldsymbol{F}} = \boldsymbol{F}_1 = \ldots = \boldsymbol{F}_n \qquad \bar{\boldsymbol{P}} = \frac{1}{\mathcal{V}} \sum_{i=1}^{N} V_i \boldsymbol{P}_i$$

Constitutive model has the capability to use microstructure character distribution data obtained by EBSD such as mean grain size and the grain orientation relationships in the form of Euler angles.

Grain interior is modelled using the following hardening model [36–42]

$$h_{\alpha\alpha} = \left\{ (h_o - h_s)\sec h^2 \left[\frac{(h_o - h_s)\gamma^{\alpha}}{\tau_s - \tau_o} \right] + h_s \right\}$$

$$h_{\alpha\beta} = q h_{\alpha\alpha} \qquad (\alpha \neq \beta)$$

As can be seen the above equation requires 4 parameters of h_o, h_s, τ_o, τ_s to be identified from experiments.

The constitutive relation for grain boundary zone is given in Figure 1. In the following, we present the list of expressions for the constitutive model without going into the detail of derivations.

The relationships for $f(\varepsilon_{ij})$ and $g(\varepsilon_{ij})$ are given below.

Before grain boundary crack initiation the following equation is dominant

$$f(\varepsilon_{ij}) = 2\left(\frac{\varepsilon_{ij}}{\mu \cdot \varepsilon_{ij,1}}\right) - \left(\frac{\varepsilon_{ij}}{\mu \cdot \varepsilon_{ij,1}}\right)^2$$

while instantly after grain boundary crack initiation the following relationships are dominant.

$$f(\varepsilon_{ij}) = \frac{e^{1-\varsigma \cdot tanh\left(\frac{\varepsilon_{ij}-\mu\cdot\varepsilon_{ij,1}}{\mu\cdot(\varepsilon_0-\varepsilon_{ij,1})}\right)^2}}{2.718} \qquad \varepsilon_{ij,1} < \varepsilon_{ij} < \varepsilon_0$$

$$g(\varepsilon_{ij}) = 2\left(\frac{\varepsilon_{ij}}{\mu\cdot\varepsilon_0}\right)^3 - 3\left(\frac{\varepsilon_{ij}}{\mu\cdot\varepsilon_0}\right)^2 + 1$$

where

$$\varepsilon_{ij,1} = Strain\ at\ \boldsymbol{\sigma}_c \qquad \varepsilon_0 = \varepsilon_{N0} = Normal\ strain\ at\ complete\ failure$$
$$\varepsilon_0 = \varepsilon_{T0} = Shear\ strain\ at\ complete\ failure$$

All simulations presented in the following are based on the code developed in the research group using FORTRAN language and all the simulations are based on local model. Total number of grains used in the model are 200. Grain misorientation was randomly distributed using experimental EBSD data reported in [46] and is not repeated have for brevity.

3. Parameter identification for type 304 austenitic stainless steel

The material data used in this analysis is a mill annealed type 304 austenitic stainless steel (UNS30400) plate with a chemical composition of (wt.%) 18.15Cr–8.60Ni–0.45Si–1.38Mn–0.055C–0.032P–0.038N–0.005S. The constitutive model requires several parameters to be determined experimentally. These are uniaxial tensile test data along with the microstructure character distribution data such as mean grain size and grain orientations. The tensile properties were obtained according to the ASTM standard for sheet, strip, flat wire and plate [43].

The HKL-EBSD system used was interfaced to a Philips XL-30 FEG-SEM. Channel 5 software was used to characterize the data, applying Brandon's criterion in the CSL model framework [44,45] to define grain boundary character. A 15◦ threshold was used to identify high angle grain boundaries (HAGB). A minimum misorientation angle of 2◦ was implemented to distinguish low angle boundaries. Grain boundaries having $\sum \leq 29$ were considered as resistant boundaries, with the low angle grain boundaries (LAGBs) ($\sum 1$) included. Information on the details of the tensile experiments and microstructure characterizations are published elsewhere [46,47].

The materials mechanical and microstructure data reported in [44] and [47] are for fully sensitized austenitic steel at room temperature. Since the experiments were performed in air the μ parameter is set to 1, i.e. no degradation of properties in the absence of corrosive environment. The identified set of parameters is listed in Table 1 and a comparison of stress-strain data is shown in Figure 2.

Table 1. Parameters identified through uniaxial tension test data on Austenitic steel at room temperature.

1(a) Grain Interior

h_0 (MPa)	τ_0 (MPa)	τ_s (MPa)	h_s (MPa)
10.	10.5	24.8	0.1

1(b) Grain Boundary

d_{gb} (mm)	N_{grain}	σ_c (MPa)	ε_0	$\varepsilon_{ij,1}$	ζ
0.005	200	1100	0.3	0.05	2.

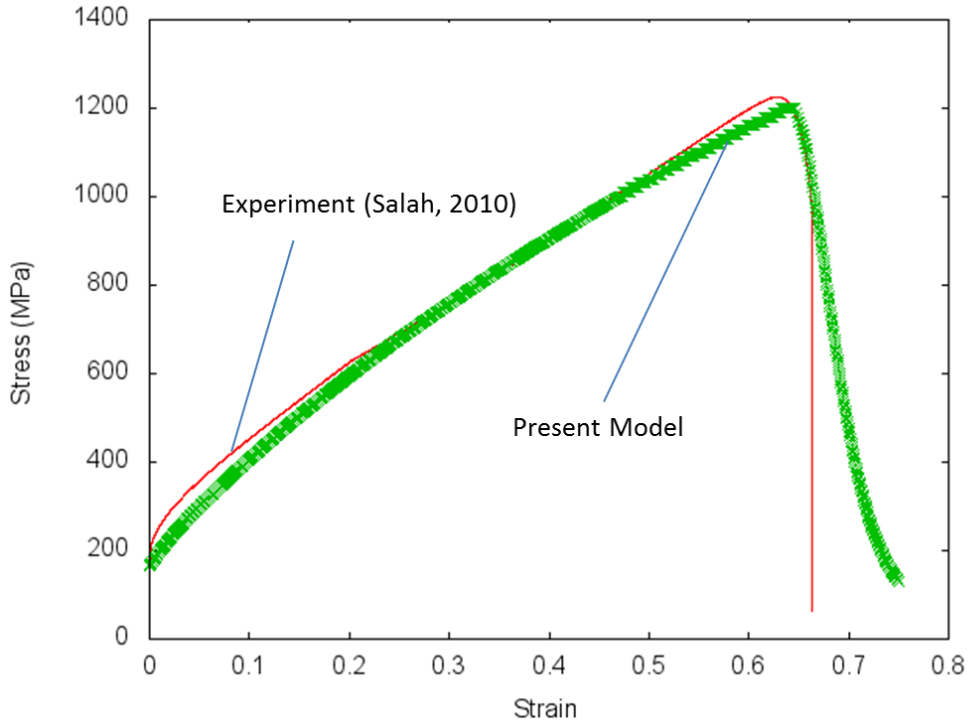

Figure 2. Comparison between uniaxial experimental [46] and simulated response of austenitic steel at room temperature

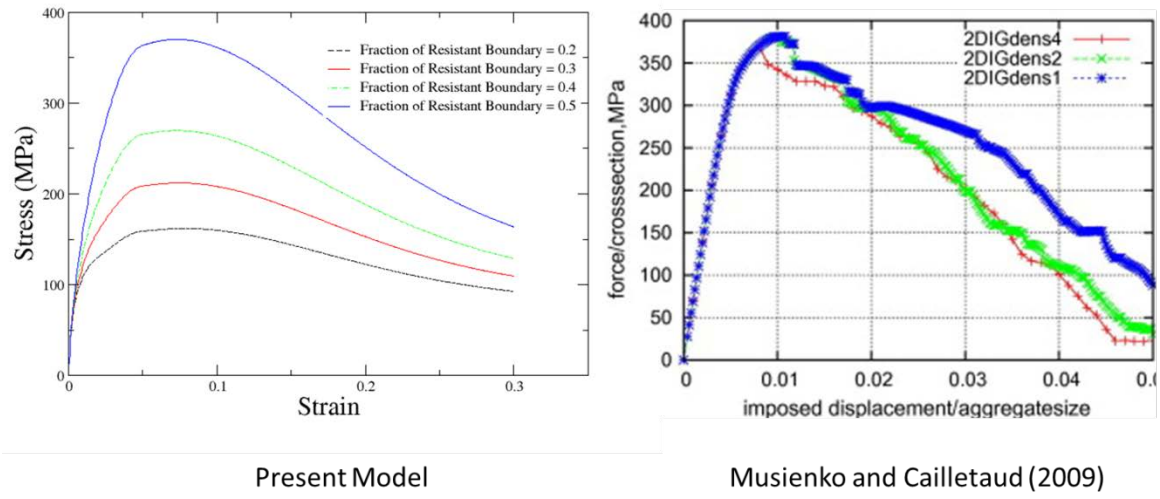

Figure 3. Effect of resistant grain boundaries number fraction (left; present model) and FE based RVE study reported in the literature (Musienko and Cailletaud [35]).

4. Model capability and validation

One of the features defined in the constitutive model is the incorporation of grain boundary characters based on their $\sum$ value, i.e. resistant and susceptible grain boundaries as has been discussed in section 3. Using these fractions of resistant and susceptible grain boundaries, constitutive model randomly distributes the grain boundaries in the representative volume of the microstructure being considered in the constitutive model. For the results discussed below parameters used are the same as Table 1 while

for μ a constant value of 0.1 is used.

To show the model capability of capturing the effect of fraction of resistant and susceptible grain boundaries, uniaxial tests were performed in the corrosive environment by assuming the value of μ equals to 0.1 for susceptible grain boundaries and 1 for resistant grain boundaries. It can be inferred from Figure 3 (left) that as the fraction of resistant grain boundary increases the failure curves shift up, i.e. material is more resistant to failure. To qualitatively compare the overall stress-strain response, finite element based RVE results on a similar material are plotted from Musienko and Cailletaud [35] which shows a very similar stress-strain response. To analyze the effect of fraction of resistant grain boundaries on crack growth rate, crack fraction as a function of time has been plotted in Figure 4 (left). It can be inferred from Figure 4 (left) that as the fraction of resistant grain boundary increases crack growth rate decreases. To qualitatively compare the overall crack growth trend, FE based RVE study reported in literature (Musienko and Cailletaud [35]) is shown in Figure 4 (right) showing overall trend in crack growth is similar.

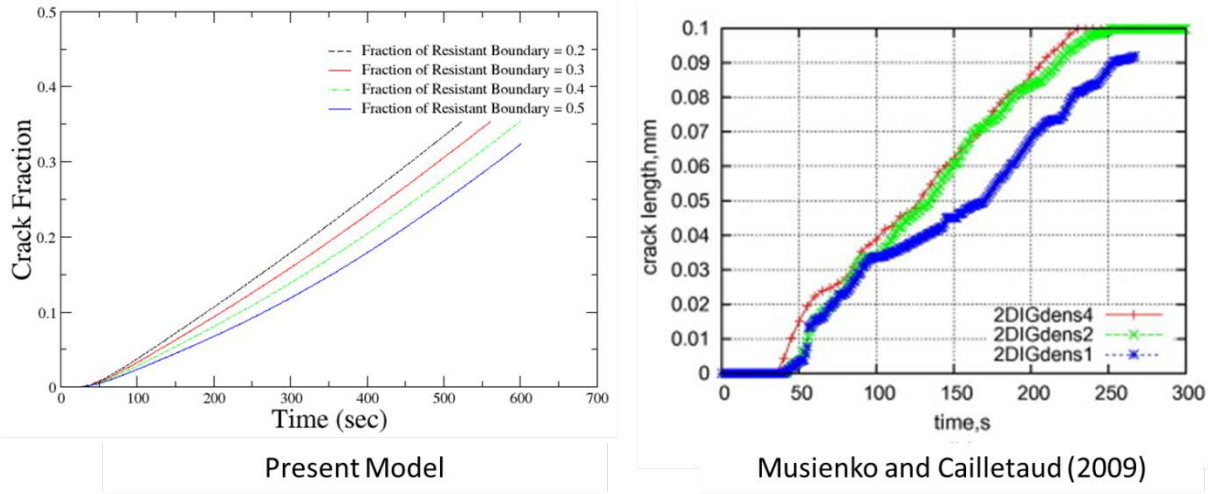

Figure 4. Effect of resistant grain boundaries number fraction on crack fraction (left; present model) and FE based RVE study reported in the literature (Musienko and Cailletaud [35]).

In order to show the effect of exposure time and load on crack growth rate, experimental double bent beam (DBB) test [46] performed on fully sensitized microstructure using constant loads of 100 and 260 MPa are simulated. Three different exposure times of 144, 288 and 432 hours were used during simulation. Based on experimental data [46] it is assumed that ζ and μ are a function of exposure time and are given by

$$\varsigma(t) = \left(\left(1 - sech^2(a_1 t)\right).b_1\right)$$
$$\mu(t) = \left(sech^2(a_1 t)\right).b_1$$

where a_1 and b_1 are material parameters to be identified from experiments.
Figure 5 shows the comparison between experimental data and simulated response. Results show a good agreement between experimental and simulated data. Parameters identified from experiments are a_1 = 0.08/hr and b_1 = 8.

5. Conclusion

We presented a multiscale constitutive model for intergranular stress corrosion cracking. Model takes into account the grain size, and grain orientation relationship using a crystal plasticity theory. Grain boundary zone is modeled using a cohesive based constitutive model. Constitutive model has the capability of using EBSD data to define grain size, orientation and distribution of grain boundary types

(resistant and susceptible). Conventional uniaxial tests in air and corrosive environment were simulated and showed a good qualitative agreement with finite element based simulations. In the last part, double bent beam experiment in corrosive environment was simulated and showed a good quantitative agreement with experimental data.

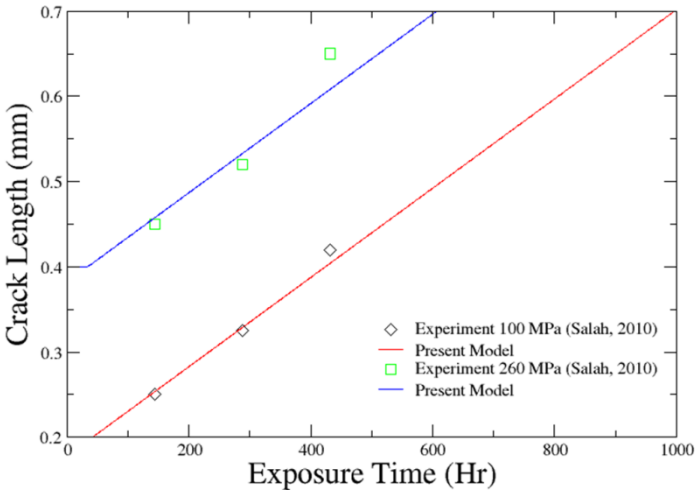

Figure 5. Crack length v/s exposure time for two different constant loads during IGSCC

References

[1] Llewellyn D and Hudd R 1998 *Steels: Metallurgy and Applications* (Boston: Butterworth Heinemann)
[2] Davis J 1994 *ASM Speciality Handbook: Stainless Steels*, (Materials Park, Ohio: ASM International)
[3] Sourmail T 2001 Review: Precipitation in Creep-Resistant Austenitic Stainless Steels *Materials Science and Technology* **17** 1–14
[4] Marshal P 1984 *Austenitic Stainless Steels, Microstructure and Mechanical Properties* (Elsevier Applied Science)
[5] Sedriks A J 1996 *Corrosion of Stainless Steels* (New York: Wiley Interscience)
[6] Parvathavarthini N 2002 Sensitisation and Testing for Intergranular Corrosion *Corrosion of Austenitic Stainless Steels. Mechanism, Mitigation and Monitoring* ed H. S. Khatak B. Raj (New Delhi: Norasa Publishing House) pp 117–38
[7] Dayal R K N, Parvathavarthini N and Raj B 2005 Influence of Metallurgical Variables on Sensitisation Kinetics in Austenitic Stainless Steels *Int. Mater. Rev.* **50** 129–55
[8] Bruemmer S M and Was G S 1994 Microstructural and microchemical mechanisms controlling intergranular stress corrosion cracking in light-water-reactor systems *J. Nucl. Mater.* **216** 348–63
[9] E8-04 A 2004 *Standard Test Methods for Tension Testing of Metallic Materials*
[10] Lehockey E M, Brennenstuhl A M and Thompson I 2004 On the relationship betweengrain boundary connectivity, coincidence site lattice boundaries and intergranular stress corrosion cracking *Corrosion Sci.* **46** 2383–404
[11] Palumbo G, King P J, Aust K T, Erb U and Lichtenberger P C 1991 Grain Boundary Design and Control for Intergranular Stress-Corrosion Resistance *Scripta Metallurgica et Materialia* **25** 1775–80
[12] Rahimi S Engelberg D L Duff J A Marrow T J 2009 In situ observation of intergranular crack nucleation in a grain boundary controlled austenitic stainless steel *J. Micros.* **233** 423–31
[13] ertsman V Y and Bruemmer S M 2001 Study of grain boundary character along intergranular stress corrosion crack paths in austenitic alloys *Acta Materialia* **49** 1589–98

[14] Stauffer D and Aharony A 1994 *Introduction to percolation theory* (London: Taylor & Francis Publication)
[15] Wells D B, Stewart J, Herbert A W, Scott P M and Williams D E 1989 The use of percolation theory to predict the probability of failure of sensitized, austenitic stainless steels by intergranular stress corrosion cracking *Corrosion* **45** 649–60
[16] Gaudett M A and Scully J R 1994 Applicability of Bond Percolation Theory to Intergranular Stress-Corrosion Cracking of Sensitised AISI 304 Stainless Steel *Metallurgical and Materials Transactions A* **25A** 775–87
[17] Pan Y, Olson T and Adams B L 1995 Application of Orientation Imaging Analysis to Microstructural Control of Intergranular Stress Corrosion Cracking *Canadian Metallurgical Quarterly* **34** 147–54
[18] Gertsman V Y and Tangri K 1997 Modelling of Intergranular Damage Propagation *Acta Materialia* **45** 4107–16
[19] Kumar M, King W E and Schwartz K J 2000 Modification to the Microstructural Topology in F.C.C Materials Through Thermomechanical Processing *Acta Materialia* **48** 2081–91
[20] Schuh C A, Kumar M and King K E 2003 Analysis of grain boundary networks and their evolution during grain boundary engineering *Acta Materialia* **51** 687–700
[21] Palumbo G, Lehockey E M Lin P 1998 Applications for grain boundary engineered materials *J. Minerals, Metals and Mater. Society* **50** 40–3
[22] Aust K T, Erb U and Palumbo G 1994 Interface control for resistance to intergranular cracking *Mater. Sci. Engng* A **176A** 329–34
[23] Lin H Pope D P 1993 The influence of grain boundary geometry on intergranular crack propagation in Ni3A1 *Acta Metallurgica et Materialia* **41** 553–62
[24] Babout L Marrow T J Engelberg D L Withers P J 2006 X-ray microtomographic observation of intergranular stress corrosion cracking in sensitised austenitic stainless steel *Mater. Sci. Technol.* **22** 1068–75
[25] Marrow T J, Babout L, Connolly B J, Engelberg D L, Johnson, G Buffiere J Y and Newman R C 2004 High Resolution in-situ, Tomographic Observations of stress corrosiobn cracking *EICM-2* vol Banff (Canada)
[26] Thomas L E Bruemmer S M 2000 High-resolution characterization of intergranular attack and stress corrosion cracking of Alloy 600 in high-temperature primary water *Corrosion* **56** 572–87
[27] McLean D 1957 *Grain boundaries in Metals* (London: Clarendon Press)
[28] Was G S Thaveeprungsriporn V Crawford D C 1998 Grain boundary misorientation effects on creep and cracking in Ni-based alloys *J. Minerals, Metals Mater. Society* **50** 44–9
[29] Palumbo G 1998 *Metal alloys having improved resistance to intergranular stress corrosion cracking* (No. 5,817,193: US patent)
[30] Gertsman V Y Janecek M Tangri K 1996 Grain boundary ensembles in polycrystals *Acta Materilia* **44** 2869–82
[31] Jivkov A P, Stevens N P C and Marrow T J 2006 A two dimensional mesoscale model for intergranular stress corrosion crack propagation *Acta Materialia* **54** 3493–501
[32] Jivkov A P, Stevens N P C and Marrow T J 2006 A three-dimensional computational model for intergranular cracking *Compiut. Mater. Sci.* **38** 442–53
[33] Jivkov A P Stevens N P C Marrow T J 2007 *Modelling of Microstructure Effects on Environment Assisted Cracking (EAC), Final Report (Modelling)* (Report Number MPC/R/051, Materials Performance Centre, School of Materials, University of Manchester)
[34] Jivkov A P and Marrow T J 2007 Rates of intergranular environment assisted cracking in three-dimensional model microstructures *Theoretical and Applied Fracture Mechanics* **48** 187–202
[35] Musienko A and Cailletaud G 2009 Simulation of inter- and transgranular crack propagation in polycrystalline aggregates due to stress corrosion cracking *Acta Materialia* **57** 3840–55

[36] Dattaguru B 2010 *IUTAM Symposium on Multi-Functional Material Structures and Systems: Proceedings of the the IUTAM Symposium on Multi-Functional Material Structures and Systems, Bangalore, India, December 10-12, 2008* vol 19 (Springer Verlag)
[37] Siddiq A and Sayed T E 2012 A thermomechanical crystal plasticity constitutive model for ultrasonic consolidation *Comput. Mater. Sci.* **51** 241–51
[38] Siddiq A and Schmauder S 2006 Interface fracture analyses of a bicrystal niobium/alumina specimen using a cohesive modelling approach *Modelling Simulation Mater. Sci. Engng* **14** 1015
[39] Siddiq A, Schmauder S and Huang Y 2007 Fracture of bicrystal metal/ceramic interfaces: a study via the mechanism-based strain gradient crystal plasticity theory *Int. J. Plasticity* **23** 665–89
[40] Siddiq A, Schmauder S and Ruehle M 2008 Niobium/alumina bicrystal interface fracture: A theoretical interlink between local adhesion capacity and macroscopic fracture energies *Engng Fracture Mech.* **75** 2320–32
[41] Siddiq A and Schmauder S 2005 Simulation of hardening in high purity niobium single crystals during deformation *Steel Grips, J. Steel Related Mater.* **3** 281–6
[42] Siddiq A and Schmauder S 2006 Crystal plasticity parameter identification procedure for single crystalline material during deformation *Journal of Computational and Applied Mechanics* **7** 1–15v
[43] Randle V 1997 No. 127-The role of the grain boundary plane in cubic polycrystals *Acta Materialia* **46** 1459–80
[44] Brandon D G 1966 The structure of high angle grain boundaries *Acta Metallurgica* **14** 1479–84
[45] Grimmer H, Bollmann W and Warrington D H 1974 Coincidence site lattice and complete pattern shift lattices in cubic crystas *Acta Crystallographica* **A30** 197–207
[46] Rahimi S 2009 *Behaviour of Short Intergranular Stress Corrosion Crack in Type 304 Austenitic Stainless Steel* (University of Manchester)
[47] Rahimi S and Marrow T J 2011 Effects of orientation, stress and exposure time on short intergranular stress corrosion crack behaviour in sensitised type 304 austenitic stainless steel *Fatigue & Fracture Engng Mater. & Struct. J.* **35** 359–73